

# Theta-3 is connected\*

Oswin Aichholzer<sup>†</sup> Sang Won Bae<sup>‡</sup> Luis Barba<sup>§ ¶</sup> Prosenjit Bose<sup>‡</sup>  
Matias Korman<sup>|| \*\*</sup> André van Renssen<sup>‡</sup> Perouz Taslakian<sup>††</sup>  
Sander Verdonschot<sup>‡</sup>

## Abstract

In this paper, we show that the  $\theta$ -graph with three cones is connected. We also provide an alternative proof of the connectivity of the Yao graph with three cones.

## 1 Introduction

Introduced independently by Clarkson [7] in 1987 and Keil [10] in 1988, the  $\theta$ -graph of a set  $P$  of points in the plane is constructed as follows. We consider each point  $p \in P$  and partition the plane into  $m \geq 2$  cones (regions in the plane between two rays originating from the same point) with apex  $p$ , each defined by two rays at consecutive multiples of  $2\pi/m$  radians from the negative  $y$ -axis; see Figure 1 for an illustration. We label the cones  $C_0$  through  $C_{m-1}$ , in clockwise order around  $p$ , starting from the cone whose angular bisector aligns with the positive  $y$ -axis from  $p$  if  $m$  is odd, or having this axis as its left boundary if  $m$  is even. If the apex is not clear from the context, we use  $C_i^p$  to denote the cone  $C_i$  with apex  $p$ . We sometimes refer to  $C_i^p$  as the  $i$ -cone of  $p$ . To build the  $\theta$ -graph, we consider each point  $p$  and connect it by an edge with the *closest* point in each of its cones. However, instead of using the Euclidean distance, we measure distance by orthogonally projecting each point onto the angle-bisector of that cone. The *closest* point to  $p$  in its  $i$ -cone is then the point in  $C_i^p$  whose projection has the smallest Euclidean distance to  $p$ .

We use this definition of distance in the remainder of the paper, except for Section 4, which deals with Yao graphs. For simplicity, we assume that no two points of  $P$  lie on a line parallel to the boundary of a cone or perpendicular to the angular bisector of a cone, guaranteeing that each point connects to at most one point in each cone. We call the  $\theta$ -graph with  $m$  cones the  $\theta_m$ -graph.

For  $\theta$ -graphs with an even number of cones, proving connectedness is easy. As the first  $m/2$  cones cover exactly the right half-plane, each point will have an edge to a point to its right, if such a point exists. Thus, we can find a path from any point to the rightmost point and, by concatenating

---

\*A preliminary version of this paper appeared in the proceedings of the 25th Canadian Conference on Computational Geometry (CCCG 2013) [1]

<sup>†</sup>Institute for Software Technology, Graz University of Technology.

<sup>‡</sup>Department of Computer Science, Kyonggi University.

<sup>§</sup>School of Computer Science, Carleton University.

<sup>¶</sup>Boursier FRIA du FNRS, Département d'Informatique, Université Libre de Bruxelles.

<sup>||</sup>National Institute of Informatics, Tokyo, Japan.

<sup>\*\*</sup>JST, ERATO, Kawarabayashi Large Graph Project.

<sup>††</sup>College of Science and Engineering, American University of Armenia.

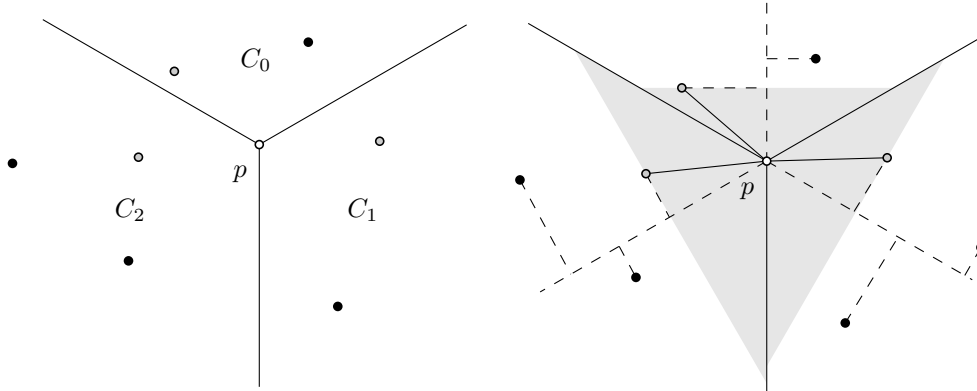


Figure 1: Left: A point  $p$  and its three cones in the  $\theta_3$ -graph. Right: Point  $p$  adds an edge to the closest point in each of its cones, where distance is measured by projecting points onto the bisector of the cone.

28 these, a path between every pair of points. Unfortunately, if  $m$  is odd this property does not hold,  
 29 as no set of cones covers *exactly* the right half-plane. Therefore, a point is not guaranteed to have  
 30 an edge to a point to its right, even if such a point exists.

31 The fact that  $\theta$ -graphs with more than 6 cones are connected has been known for a long time.  
 32 In fact, they even guarantee the existence of a *short* path between every pair of points. The length  
 33 of this path is bounded by a constant times the straight-line Euclidean distance between the two  
 34 points [4, 6, 7, 10, 12]. Graphs that have this property are called *geometric spanners*. For more  
 35 information on geometric spanners, see the book by Narasimhan and Smid [11].

36 For a long time, very little was known about  $\theta$ -graphs with fewer than 7 cones. Bonichon *et*  
 37 *al.* [3] broke ground in this area in 2010, by showing that the  $\theta_6$ -graph is a geometric spanner. Sub-  
 38 sequently, both the  $\theta_4$ - and  $\theta_5$ -graphs have been shown to be geometric spanners [2, 5]. El Molla [9]  
 39 already showed that the  $\theta_2$ - and  $\theta_3$ -graphs are not geometric spanners. It is straightforward to  
 40 verify that the  $\theta_2$ -graph is connected which leaves the  $\theta_3$ -graph as the only  $\theta$ -graph for which con-  
 41 nectedness has not been proven. In this paper, we settle this question by showing that the  $\theta_3$ -graph  
 42 is always connected.

43 The question of connectedness about the  $\theta_3$ -graph is interesting because the  $\theta_3$ -graph has some  
 44 unique properties that cause standard proof techniques for  $\theta$ -graphs to fail. As such, we hope that  
 45 the techniques we develop here will lead to more insight into the structure of other  $\theta$ -graphs. As  
 46 an example, most proofs for a larger number of cones show that the  $\theta$ -routing algorithm (always  
 47 follow the edge to the closest vertex in the cone that contains the destination) returns a short  
 48 path between any two points. But in the  $\theta_3$ -graph,  $\theta$ -routing is not guaranteed to ever reach the  
 49 destination. The smallest point set that exhibits this behavior has three points, such that for each  
 50 point, both other points lie in the same cone; see Figure 2. In fact, this example shows not only  
 51 that this exact routing strategy fails; it shows that if we consider the edges to be directed (from  
 52 the point that added them, to the closest point in its cone), the graph is not strongly connected.  
 53 Therefore, our proof requires more global methods than previous proofs on  $\theta$ -graphs.

54 Most proofs for a larger number of cones use induction on the distance between points or on the  
 55 size of the empty triangle between a point and its closest point. In the  $\theta_3$ -graph however, both of  
 56 these measures can increase when we follow an edge. Thus, applying induction on these distances  
 57 seems a difficult task. An induction on the number of points similarly fails, as inserting a new point

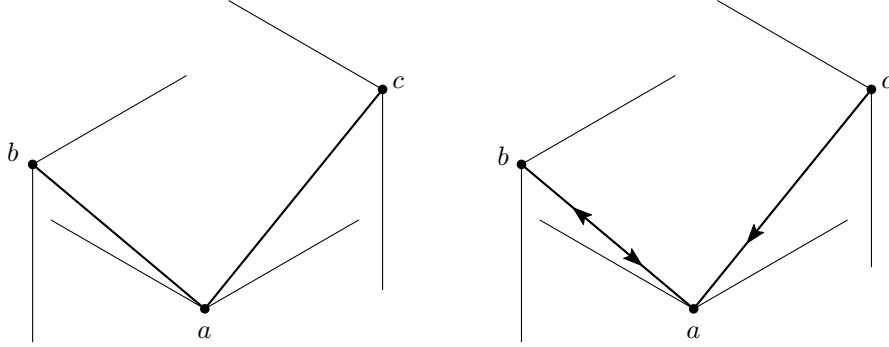


Figure 2: Left: A point set for which  $\theta$ -routing does not find a path from  $a$  to  $c$ , as it keeps cycling between  $a$  and  $b$ . Right: The directed version of the graph is not strongly connected, as there is no path from either  $a$  or  $b$  to  $c$ .

58 may remove edges that were present before, and it is not obvious that the endpoints of those edges  
 59 are still connected in the new graph.

60 The  $\theta_3$ -graph is strongly related to the  $Y_3$ -graph, where each point also connects to the closest  
 61 point in each cone, but the distance measure is the standard Euclidean distance. This graph was  
 62 shown to be connected by Damian and Kumbhar [8]. Their proof uses induction on a rhomboid  
 63 distance-measure that was tailored specifically for the  $Y_3$ -graph. Since the ‘closest’ point for the  $\theta_3$ -  
 64 graph can be much further away than in the  $Y_3$ -graph, this method of induction does not translate  
 65 to the  $\theta_3$ -graph, either. Conversely, we show that our proof extends to the  $Y_3$ -graph, providing an  
 66 alternative proof for its connectivity.

## 67 2 Properties of the $\theta_3$ -graph

68 For  $i \in \{0, 1, 2\}$ , the edge connecting a point with its closest point in cone  $C_i$  is called an  $i$ -edge.  
 69 Note that an edge can have one or two roles depending on the position of its endpoints. An example  
 70 is depicted in Figure 2, where edge  $ab$  is both the 0-edge of  $a$  and the 1-edge of  $b$ .

71 **Lemma 1.** For all  $i \in \{0, 1, 2\}$ , no two  $i$ -edges of the  $\theta_3$ -graph can cross.

72 *Proof.* We consider only 0-edges of  $P$ ; the proof is analogous for 1- and 2-edges. For a contradiction,  
 73 assume that there are two 0-edges that cross at a point  $s$ . Call these edges  $u_1v_1$  and  $u_2v_2$ , such  
 74 that  $v_1$  is in the 0-cone of  $u_1$  and  $v_2$  in the 0-cone of  $u_2$ . Assume without loss of generality that  
 75 the  $y$ -coordinate of  $v_1$  is smaller than that of  $v_2$ ; see Figure 3 for an illustration. Because  $s$  lies  
 76 on segments  $u_1v_1$  and  $u_2v_2$ ,  $s$  lies in the 0-cones of both  $u_1$  and  $u_2$ . Therefore, the 0-cone of  $s$   
 77 is contained in the intersection of the 0-cones of  $u_1$  and  $u_2$ . As  $v_1$  lies in cone  $C_0$  of  $s$ , point  $v_1$   
 78 lies in cone  $C_0$  of  $u_2$  as well. Because we assumed that the  $y$ -coordinate of  $v_1$  is less than that of  
 79  $v_2$ , we conclude that  $v_1$  is closer to  $u_2$  than  $v_2$ . Thus, the edge  $u_2v_2$  is not a 0-edge, yielding a  
 80 contradiction.  $\square$

81 We say that a cone is *empty* if it contains no point of  $P$  in its interior. A point having an empty  
 82  $i$ -cone is called an  $i$ -sink.

83 Given a point  $p$  of  $P$ , the  $i$ -path from  $p$  is defined recursively as follows: If the  $i$ -cone of  $p$  is  
 84 empty, the  $i$ -path from  $p$  consists of the single point  $p$ . Otherwise, let  $q$  be the closest point to  $p$  in  
 85 its  $i$ -cone. The  $i$ -path from  $p$  is defined as the union of edge  $pq$  with the  $i$ -path from  $q$ .

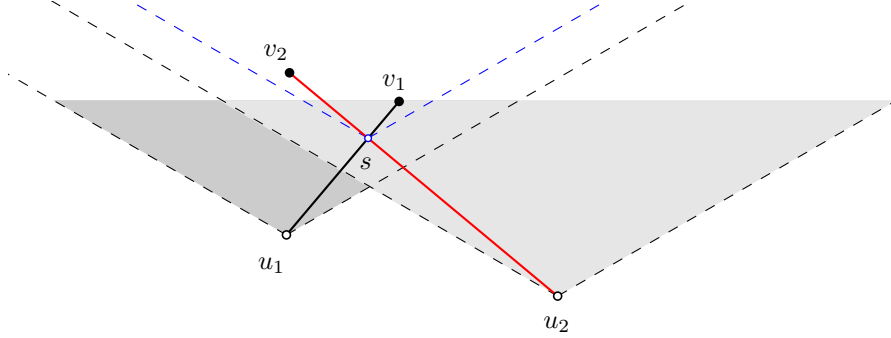


Figure 3: Two 0-edges  $u_1v_1$  and  $u_2v_2$  such that  $v_1 \in C_0^{u_1}$  and  $v_2 \in C_0^{u_2}$  cannot cross because the lowest point among  $v_1$  and  $v_2$  will be adjacent to both  $u_1$  and  $u_2$ .

86 **Lemma 2.** *Every  $i$ -path of the  $\theta_3$ -graph is well-defined and has an  $i$ -sink at one of its endpoints.*

87 *Proof.* We consider only 0-paths; the proof is analogous for the other paths. A 0-path from a point  
 88  $p$  is well defined because the closest point in the 0-cone of  $p$  always lies above  $p$ . Therefore, the  
 89  $y$ -coordinates of the points in the 0-path from  $p$  form a monotonically increasing sequence. As  $P$   
 90 is a finite set, the recursion must end at a point having an empty 0-cone.  $\square$

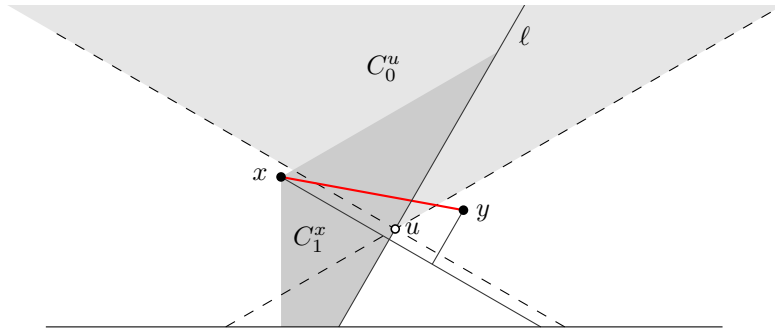


Figure 4: Empty cones cannot be crossed by edges of the  $\theta_3$ -graph.

91 **Lemma 3.** *If a cone of a point is empty, then no edge of the  $\theta_3$ -graph can cross this cone.*

92 *Proof.* We consider only 0-cones for this proof; analogous arguments hold for the other cones. Let  
 93  $u$  be a point of  $P$  with an empty 0-cone. For a contradiction, assume that there exists an edge  
 94  $xy$  that crosses  $C_0^u$ . For this to happen,  $x$  and  $y$  have to lie in opposite sectors of the double  
 95 wedge obtained by extending the boundary segments of  $C_0^u$ ; see Figure 4. Assume without loss of  
 96 generality that  $x$  lies in the left wedge. Then  $x$  lies in  $C_2^u$  while  $y$  lies in  $C_1^u$ . In particular, this  
 97 implies that both  $u$  and  $y$  lie in  $C_1^x$ .

98 Let  $\ell$  be the line through  $u$  perpendicular to the bisector of  $C_1^x$ . For the edge  $xy$  to exist, the  
 99 projection of  $y$  on the bisector of  $C_1^x$  must be closer to  $x$  than the projection of  $u$ . In other words,  $y$   
 100 must lie to the left of  $\ell$ . However, all points lying to the left of  $\ell$  are contained in  $C_0^u \cup C_2^u$ , yielding  
 101 a contradiction as  $y \in C_1^u$ .  $\square$

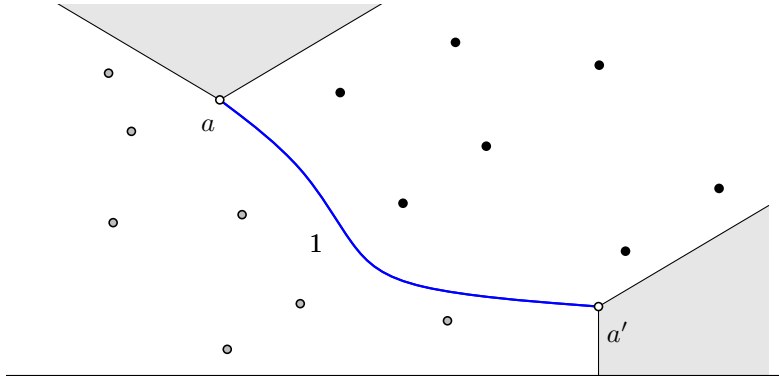


Figure 5: A 1-barrier, defined by the 1-path joining  $a$  with  $a'$ , splits the remaining points into two sets such that no two points in different sets can be joined by a 1-path.

102 As a consequence of Lemmas 1 and 3, two sinks connected by an  $i$ -path partition the remaining  
 103 points into two sets such that no  $i$ -path can connect a point in one set to a point in the other set,  
 104 as any such path would cross either the  $i$ -path between the sinks, or the empty cone of one of the  
 105 sinks. Such a construction is called an  $i$ -barrier; see Figure 5 for an illustration.

### 106 3 Proving connectedness

107 In this section we prove that the  $\theta_3$ -graph of any given point set is connected. We start by proving  
 108 that three given 0-sinks in a specific configuration are always connected. We then prove that if the  
 109  $\theta_3$ -graph has at least two disjoint connected components, there exist three 0-sinks that are in this  
 110 configuration and are not all in the same component, leading to a contradiction.

111 Although the edges of the  $\theta_3$ -graph are not directed, by Lemma 2 we can think of an  $i$ -path  
 112 as oriented towards the  $i$ -sink it reaches. An  $i$ -path from  $a$  that ends at an  $i$ -sink  $b$  is denoted by  
 113  $a \rightarrow b$ . The following lemma is depicted in Figure 6.

114 **Lemma 4.** *Let  $a$ ,  $b$ , and  $c$  be three 0-sinks such that (i)  $a$  lies to the left of  $b$  and  $b$  lies to the left*  
 115 *of  $c$ , and (ii) the 1-path from  $a$  ends at a 1-sink  $a'$  whose 0-path ends at  $c$  ( $a'$  may be equal to  $c$ ).*  
 116 *Then,  $a$ ,  $b$ , and  $c$  belong to the same connected component.*

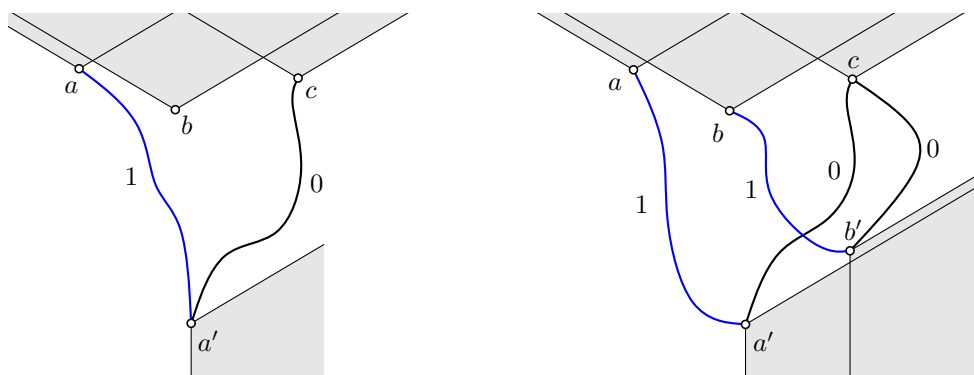


Figure 6: Left: The configuration of points described in Lemma 4. Right: The configuration in the base case of the induction where no 0-sink lies to the right of  $c$ .

117 *Proof.* Because there is a path from  $a$  to  $c$  via  $a'$ ,  $a$  and  $c$  must be in the same component. We  
 118 show that  $b$  belongs to this same connected component.

119 The proof proceeds by induction on the number of 0-sinks to the right of  $c$ . In the base case,  
 120 there are no 0-sinks to the right of  $c$ . Consider the 1-sink  $b'$  at the end of the 1-path from  $b$ ; see  
 121 Figure 6 (right). Because the 1-path  $a \rightarrow a'$  forms a 1-barrier,  $b'$  cannot lie to the left of  $a'$ .

122 If  $a' = c$ , then  $a'$  is both a 1-sink and a 0-sink. This means that there can be no points to the  
 123 right of  $a'$ . Therefore  $b'$  must also be equal to  $a'$ . But then  $b$  is in the same connected component as  
 124  $a$  and we are done. So assume that this is not the case, that is,  $a' \neq c$  and  $b'$  lies to the right of  $a'$ .

125 Then the 1-path  $b \rightarrow b'$  also has to cross the 0-path  $a' \rightarrow c$ , as otherwise  $a' \rightarrow c$  crosses the  
 126 empty cone of  $b'$ , which is impossible by Lemma 3, or  $b'$  lies on  $a' \rightarrow c$  and we are done. Moreover,  
 127 because  $a' \rightarrow c$  forms a 0-barrier, the 0-path from  $b'$  cannot end to the left of  $c$ . However, since  
 128 there are no 0-sinks to the right of  $c$ , the 0-path from  $b'$  must end at  $c$ . Thus, there is a path  
 129 connecting  $b$  and  $c$ , which proves the lemma in the base case.

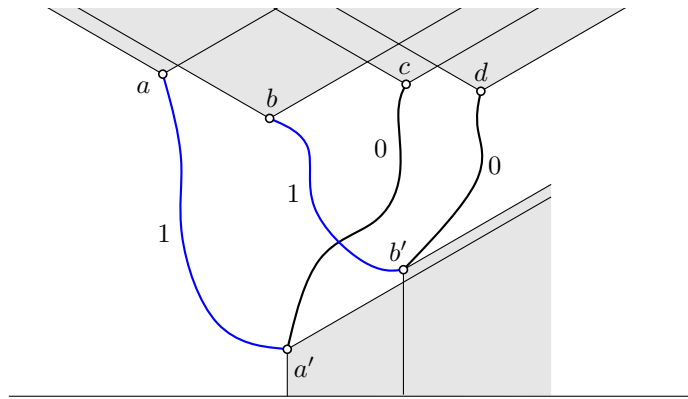


Figure 7: The configuration of the inductive step where the induction hypothesis can be applied on 0-sinks  $b$ ,  $c$  and  $d$ .

130 For the inductive step, let  $k$  be the number of 0-sinks to the right of  $c$  and assume that the  
 131 lemma holds for any triple of 0-sinks with fewer than  $k$  0-sinks to their right. By the same argument  
 132 as in the base case, we have a 1-path from  $b$  to a 1-sink  $b'$  that lies to the right of  $a'$ . Now consider  
 133 the 0-sink  $d$  at the end of the 0-path from  $b'$ ; see Figure 7. Note that  $b'$  and  $d$  could be the same  
 134 vertex.

135 Since the 0-path  $a' \rightarrow c$  forms a 0-barrier,  $d$  cannot lie to the left of  $c$ . If  $d$  and  $c$  are the same  
 136 point, we have a path connecting  $b$  and  $c$  as in the base case, so assume that this is not the case.  
 137 Thus  $d$  lies to the right of  $c$ . Now  $b$ ,  $c$ , and  $d$  form a triple of 0-sinks that satisfy criteria (i) and (ii).  
 138 And since  $d$  is a 0-sink to the right of  $c$ , there are fewer than  $k$  0-sinks to the right of  $d$ . Thus, by  
 139 induction, we have that  $b$  is in the same connected component as  $c$ , which proves the lemma.  $\square$

140 **Theorem 5.** *The  $\theta_3$ -graph is connected.*

141 *Proof.* Assume for a contradiction that there exists a point set  $P$  whose  $\theta_3$ -graph  $G$  is not connected.  
 142 From each point, we can follow its 0-path to a 0-sink. Therefore,  $G$  must contain at least one 0-sink  
 143 for each connected component. Let  $a$  be the leftmost 0-sink, and let  $A$  be the connected component  
 144 of  $G$  that contains  $a$ . Now let  $b$  be the leftmost 0-sink that does not belong to  $A$ .

145 We use Lemma 4 to show that, in fact,  $b$  must belong to  $A$  as well. Before we can do this, we  
 146 need to define two barriers. The first barrier is formed by the 2-path from  $b$ , ending at a 2-sink

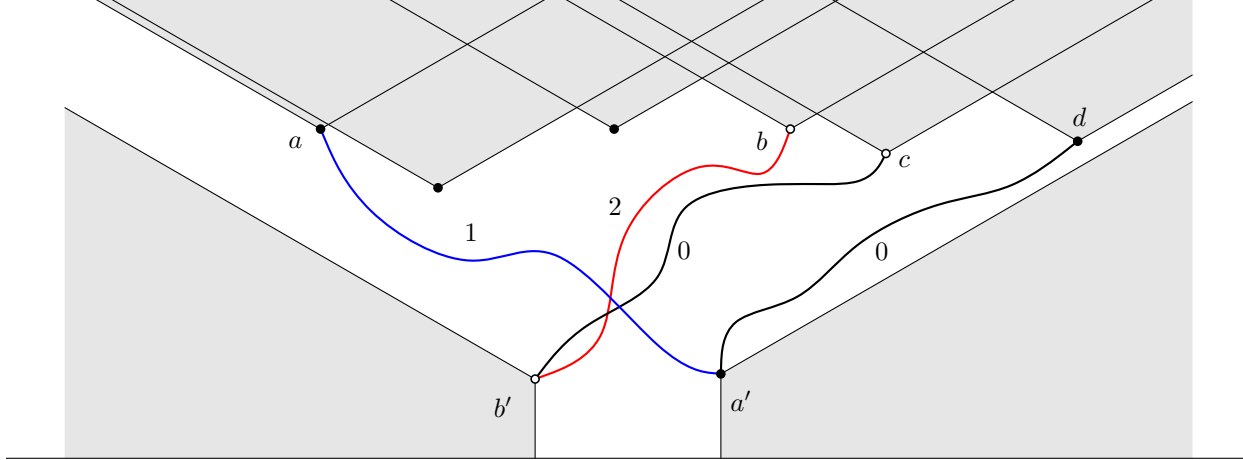


Figure 8: Two 0-sinks  $a$  and  $b$  are assumed to lie in different components such that both  $a$  and  $b$  are the leftmost 0-sinks in their component. The 1-path from  $a$  ends at a 1-sink  $a'$  whose 0-path ends at a 0-sink  $d$  lying to the right of  $b$ . The 0-sinks  $a, b$  and  $d$  jointly satisfy the criteria of Lemma 4.

147  $b'$ . Because  $a$  lies in  $C_2^b$ , point  $b$  does not have an empty 2-cone and hence,  $b'$  differs from  $b$ . The  
 148 second barrier is formed by the 0-path from  $b'$ , which ends at a 0-sink  $c$ ; see Figure 8. Since  $b$  is  
 149 the leftmost 0-sink that does not belong to  $A$ , either  $c$  and  $b$  are the same point, or  $c$  lies to the  
 150 right of  $b$ .

151 Now consider the 1-sink  $a'$  at the end of the 1-path from  $a$ . This point has to lie to the right  
 152 of both barriers  $b \rightarrow b'$  and  $b' \rightarrow c$ , as otherwise these paths would cross the empty cone  $C_1$  of  $a'$ ,  
 153 which is not allowed by Lemma 3. Because the path  $a \rightarrow a'$  is a 1-path and the barriers in question  
 154 consist of 0- and 2-edges, these crossings are possible. Now let  $d$  be the 0-sink at the end of the  
 155 0-path from  $a'$ . Since this path cannot cross the 0-barrier  $b' \rightarrow c$ ,  $d$  cannot lie to the left of  $c$ .

156 Because  $d$  belongs to component  $A$ , if  $c$  and  $d$  are the same point,  $c$  belongs to component  $A$ .  
 157 Otherwise, if  $c$  and  $d$  are distinct points, then  $a, b$ , and  $d$  jointly satisfy the criteria of Lemma 4,  
 158 which gives us that  $b$  belongs to component  $A$  as well—a contradiction since  $b$  is the leftmost 0-sink  
 159 that does not belong to  $A$ . This contradiction comes from our assumption that  $G$  is not connected.  
 160 Therefore, the  $\theta_3$ -graph of any point set is connected.  $\square$

## 161 4 The $Y_3$ -graph

162 The construction of the  $Y_3$ -graph is very similar to that of the  $\theta_3$ -graph. The only difference is the  
 163 way distance is measured: the  $\theta$ -graph uses the length of the projection onto the bisector, whereas  
 164 the Yao graph uses the Euclidean distance. Therefore, in every cone a point is connected to its  
 165 closest Euclidean neighbor. We denote by  $|pq|$  the Euclidean distance between two points  $p$  and  $q$ .

166 We show that, like the  $\theta_3$ -graph, the  $Y_3$ -graph is connected. To this end, we re-introduce  
 167 the three basic lemmas we had for the  $\theta_3$ -graph and show that the same properties hold for the  
 168  $Y_3$ -graph. We first prove a geometric auxiliary lemma depicted in Figure 9.

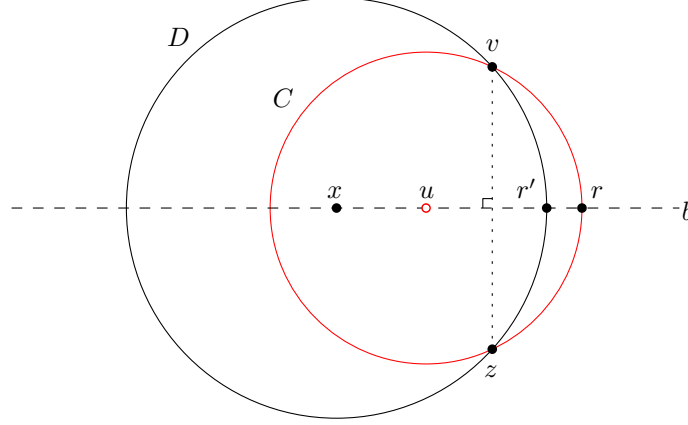


Figure 9: Point  $x$  lies to the left of point  $u$  and the arcs  $vr'$  and  $r'z$  are enclosed by circle  $C$  centered at  $u$ , having radius  $|uv|$ .

169 **Lemma 6.** *Given a non-vertical line  $b$  and a circle  $C$  centered at a point  $u$  on  $b$ , let  $v$  and  $z$  be*  
 170 *two points on  $C$  such that  $b$  bisects the segment  $vz$ . Let  $x$  be a point on  $b$  and let  $D$  be the circle*  
 171 *centered at  $x$  with radius  $|xv|$ . If  $x$  lies to the left of  $u$ , then the right-side arc of  $D$  between  $v$  and*  
 172  *$z$  is enclosed by  $C$ ; otherwise, the left-side arc of  $D$  between  $v$  and  $z$  is enclosed by  $C$ .*

173 *Proof.* Assume that  $x$  lies to the left of  $u$ ; the proof of the other case is analogous. Let  $r$  and  $r'$  be  
 174 the respective right intersections of  $C$  and  $D$  with line  $b$ ; see Figure 9. Hence, arcs  $vr'$  and  $r'z$  lie  
 175 either entirely inside  $C$  or entirely outside  $C$ . Therefore, it suffices to show that  $r'$  lies inside  $C$ ,  
 176 i.e.,  $|ur'| \leq |ur|$ . Since  $x$  lies to the left of  $u$ , we can rewrite  $|ur'|$  as  $|xr'| - |xu|$ . Since  $|xr'| = |xv|$   
 177 and  $|ur| = |uv|$ , we thus need to show that  $|xv| \leq |xu| + |uv|$ . This follows from the triangle  
 178 inequality.  $\square$

179 The proof of the following lemma is similar to that of Lemma 1.

180 **Lemma 7.** *For all  $i \in \{0, 1, 2\}$ , no two  $i$ -edges of the  $Y_3$ -graph can cross.*

181 *Proof.* We look at the 0-edges. The cases for the other edges are analogous. Let  $uv$  be a 0-edge  
 182 such that  $v \in C_0^u$  and assume without loss of generality that  $v$  lies to the right of  $u$ . We prove the  
 183 lemma by contradiction, so assume that some 0-edge  $xy$  crosses  $uv$  and let  $y \in C_0^x$ . Note that for  
 184  $xy$  to cross  $uv$ ,  $C_0^x$  must contain some part of  $uv$ . Hence  $v$  lies in  $C_0^x$ .

185 Let  $k$  be the line through the right boundary of  $C_0^u$  and let  $l$  be the line through  $u$ , perpendicular  
 186 to  $k$ . We consider four cases, depending on the location of  $x$  with respect to  $u$ ; see Figure 10 (left):  
 187 (a)  $x \in C_0^u$  to the left of the line  $uv$ , (b)  $x \in C_2^u$  above  $k$ , (c)  $x \in C_2^u$  below  $k$  or  $x \in C_1^u$  below  $l$ ,  
 188 (d)  $x \in C_1^u$  above  $l$  or  $x \in C_0^u$  to the right of the line  $uv$ .

189 **Case (a):**  $x \in C_0^u$  to the left of the line  $uv$ . Since  $v$  lies inside  $C_0^x$  and  $v$  lies to the right of  $u$ ,  
 190  $x$  lies in the circle centered at  $u$  having radius  $|uv|$ . Thus,  $x$  lies closer to  $u$  than  $v$ , contradicting  
 191 the existence of edge  $uv$ .

192 **Case (b):**  $x \in C_2^u$  above  $k$ . We apply Lemma 6 as follows, see Figure 10 (right): Let  $C$  be  
 193 the circle centered at  $u$  having radius  $|uv|$ . Let  $b$  be the line through  $u$  and  $x$ , and let  $z$  be the  
 194 reflection of  $v$  in  $b$ . Note that this implies that  $z$  lies outside  $C_0^u$ . Let  $D$  be the circle centered at  
 195  $x$  having radius  $|xv|$ . Since  $x$  lies to the left of  $u$ , Lemma 6 gives us that the right arc  $vz$  of circle



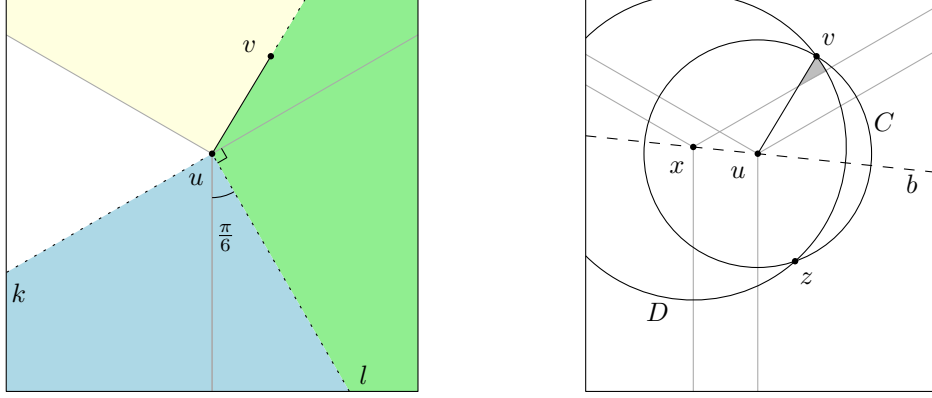


Figure 10: Left: The four cases. Right: The case when  $x$  lies in  $C_2^u$  and above  $k$ .

196  $D$  is enclosed by circle  $C$ . Since the area in which  $y$  must lie for  $xy$  to cross  $uv$  is bounded by the  
 197 right boundary of  $C_0^x$ , edge  $uv$ , and the right arc  $vz$  of circle  $D$ , it is enclosed by  $C$ . Therefore, any  
 198 such point would lie in  $C_0^u$  and be closer to  $u$  than  $v$ , contradicting the existence of edge  $uv$ .

199 **Case (c):**  $x \in C_2^u$  below  $k$  or  $x \in C_1^u$  below  $l$ ; see Figure 11 (left). Since  $u$  lies in  $C_0^x$ ,  $y$  needs  
 200 to be closer to  $x$  than  $u$  for edge  $xy$  to exist. Hence it must lie inside the circle  $C$  centered at  $x$   
 201 with radius  $|xu|$ . Look at the lower half-plane defined by the line tangent to  $C$  at  $u$  and note that  
 202  $C$  is contained in this half-plane. However, the half-plane does not intersect  $C_0^u$  to the right of  $u$   
 203 and hence no point  $y$  inside the half-plane can be used to form an edge  $xy$  that crosses  $uv$ .

204 **Case (d):**  $x \in C_1^u$  above  $l$  or  $x \in C_0^u$  to the right of the line  $uv$ . We apply Lemma 6 as follows,  
 205 see Figure 11 (right): Let  $C$  be the circle centered at  $u$  having radius  $|uv|$ . Let  $b$  be the line through  
 206  $u$  and  $x$ , and let  $z$  be the reflection of  $v$  in  $b$ . Note that  $z$  lies outside  $C_0^x$ . Let  $D$  be the circle  
 207 centered at  $x$  having radius  $|xv|$ . Since  $x$  lies to the right of  $u$ , Lemma 6 gives us that the left  
 208 arc  $vz$  of circle  $D$  is enclosed by circle  $C$ . Since the area in which  $y$  must lie for  $xy$  to cross  $uv$  is  
 209 bounded by edge  $uv$ , the left arc  $vz$  of circle  $D$ , and either the left boundary of  $C_0^x$  (if  $u \notin C_0^x$ ) or  
 210 the line  $ux$  (if  $u \in C_0^x$ ), it is enclosed by  $C$ . Therefore, there does not exist a point  $y \in C_0^x$  such  
 211 that  $xy$  intersects  $uv$ .  $\square$

212 **Lemma 8.** Every  $i$ -path of the  $Y_3$ -graph is well-defined and has an  $i$ -sink as one of its endpoints.

213 *Proof.* The proof of this lemma is analogous to Lemma 2 for the  $\theta_3$ -graph.  $\square$

214 **Lemma 9.** If a cone of a point is empty, then no edge in the  $Y_3$ -graph can cross this cone.

215 *Proof.* We assume without loss of generality that  $C_0^u$  does not contain any points. We prove the  
 216 lemma by contradiction, so assume that there exists an edge  $xy$  that crosses  $C_0^u$ . Since no edge  
 217 between two points in the same cone can cross another cone, let  $x \in C_2^u$  and  $y \in C_1^u$ .

218 Point  $y$  cannot lie in  $C_0^x$ , since either  $C_0^x$  does not intersect  $C_1^u$  (if  $u \notin C_0^x$ ) or the line segment  
 219 between  $x$  and  $y$  does not intersect  $C_0^u$  (if  $u \in C_0^x$ ). Hence  $y$  must lie in  $C_1^x$ .

220 If  $u \in C_0^x$ ,  $C_1^x$  does not intersect  $C_0^u$  and thus the line segment between  $x$  and  $y$  cannot intersect  
 221  $C_0^u$  either. Therefore both  $u$  and  $y$  lie in  $C_1^x$ . Let  $C$  be the circle centered at  $x$  with radius  $|xu|$ .  
 222 For the edge  $xy$  to exist,  $y$  must be closer to  $x$  than  $u$ , which means that  $y$  must lie in  $C$ . Note  
 223 that  $C$  is contained in the half-plane to the left of the tangent to  $C$  at  $u$ .

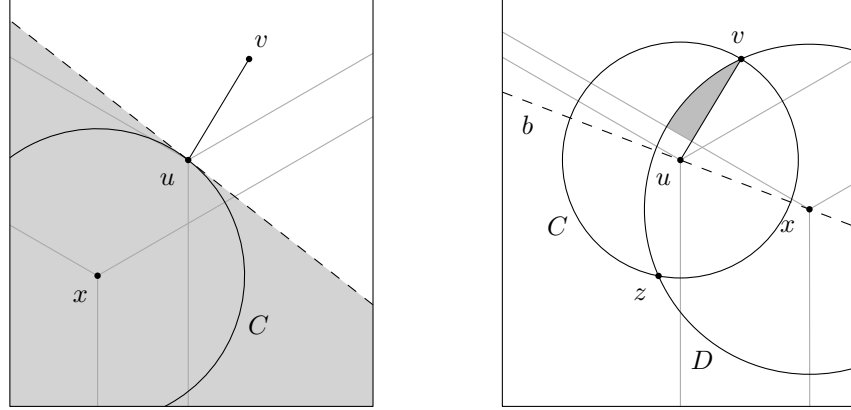


Figure 11: Left: The case when  $x \in C_2^u$  below  $k$  or  $x \in C_1^u$  below  $l$ . Right: The case when  $x \in C_1^u$  above  $l$  or  $x \in C_0^u$  to the right of the line  $uv$ .

224 If  $x$  lies on or above the horizontal line through  $u$ , the half-plane does not intersect  $C_1^u$ . If  $x$   
 225 lies below the horizontal line through  $u$ , the half-plane does not intersect  $C_1^u$  above  $u$  and thus  $xy$   
 226 would not cross  $C_0^u$ . Since  $y$  is enclosed by  $C$ ,  $C$  is contained in the half-plane, and there is no  
 227 point  $p$  in the half-plane such that  $p \in C_1^u$  and  $px$  crosses  $C_0^u$ ,  $xy$  cannot cross  $C_0^u$  either.  $\square$

228 Using Lemmas 7, 8 and 9, the proof of Theorem 5 translates directly to the  $Y_3$ -graph yielding  
 229 the following result.

230 **Theorem 10.** *The  $Y_3$ -graph is connected.*

231 **Acknowledgments.** This problem was introduced during the 2012 Fields Workshop on Discrete  
 232 and Computational Geometry held at Carleton University in Ottawa, Canada. The research of  
 233 Oswin Aichholzer was partially supported by the ESF EUROCORES programme EuroGIGA - CRP  
 234 ‘ComPoSe’, Austrian Science Fund (FWF): I648-N18. Work by Sang Won Bae was supported by  
 235 the Contents Convergence Software Research Center funded by the GRRC Program of Gyeonggi  
 236 Province, South Korea. The research of Luis Barba, Prosenjit Bose, André van Renssen, and  
 237 Sander Verdonschot was supported in part by NSERC. Matias Korman received support from  
 238 the Secretary for Universities and Research of the Ministry of Economy and Knowledge of the  
 239 Government of Catalonia, the European Union, and projects MINECO MTM2012-30951, Gen.  
 240 Cat. DGR2009SGR1040, ESF EUROCORES programme EuroGIGA – CRP ‘ComPoSe’: MICINN  
 241 Project EUI-EURC-2011-4306.

## 242 References

- 243 [1] O. Aichholzer, S. W. Bae, L. Barba, P. Bose, M. Korman, A. van Renssen, P. Taslakian, and  
 244 S. Verdonschot. Theta-3 is connected. In *Proceedings of the 25th Canadian Conference on*  
 245 *Computational Geometry (CCCG 2013)*, pages 205–210, 2013.
- 246 [2] L. Barba, P. Bose, J.-L. De Carufel, A. van Renssen, and S. Verdonschot. On the stretch factor  
 247 of the Theta-4 graph. In *Proceedings of the 13th Algorithms and Data Structures Symposium*  
 248 *(WADS 2013)*, pages 109–120, 2013.

- 249 [3] N. Bonichon, C. Gavoille, N. Hanusse, and D. Ilcinkas. Connections between theta-graphs,  
250 Delaunay triangulations, and orthogonal surfaces. In *Proceedings of the 36th International*  
251 *Workshop on Graph Theoretic Concepts in Computer Science (WG 2010)*, pages 266–278,  
252 2010.
- 253 [4] P. Bose, J.-L. De Carufel, P. Morin, A. van Renssen, and S. Verdonschot. Optimal bounds on  
254 theta-graphs: More is not always better. In *Proceedings of the 24th Canadian Conference on*  
255 *Computational Geometry (CCCG 2012)*, pages 305–310, 2012.
- 256 [5] P. Bose, P. Morin, A. van Renssen, and S. Verdonschot. The  $\theta_5$ -graph is a spanner. In  
257 *Proceedings of the 39th International Workshop on Graph-Theoretic Concepts in Computer*  
258 *Science (WG 2013)*, pages 100–114, 2013.
- 259 [6] P. Bose, A. van Renssen, and S. Verdonschot. On the spanning ratio of theta-graphs. In  
260 *Proceedings of the 13th Algorithms and Data Structures Symposium (WADS 2013)*, pages  
261 182–194, 2013.
- 262 [7] K. L. Clarkson. Approximation algorithms for shortest path motion planning. In *Proceedings*  
263 *of the 19th ACM Symposium on the Theory of Computing (STOC 1987)*, pages 56–65, 1987.
- 264 [8] M. Damian and A. Kumbhar. Undirected connectivity of sparse yao graphs. In *Proceedings*  
265 *of the 7th ACM SIGACT/SIGMOBILE International Workshop on Foundations of Mobile*  
266 *Computing (FOMC 2011)*, pages 25–32, 2011.
- 267 [9] N. M. El Molla. *Yao spanners for wireless ad hoc networks*. PhD thesis, Villanova University,  
268 2009.
- 269 [10] J. M. Keil. Approximating the complete Euclidean graph. In *Proceedings of the 1st Scandina-*  
270 *vian Workshop on Algorithm Theory (SWAT 1988)*, pages 208–213, 1988.
- 271 [11] G. Narasimhan and M. Smid. *Geometric Spanner Networks*. Cambridge University Press,  
272 2007.
- 273 [12] J. Ruppert and R. Seidel. Approximating the  $d$ -dimensional complete Euclidean graph. In  
274 *Proceedings of the 3rd Canadian Conference on Computational Geometry (CCCG 1991)*, pages  
275 207–210, 1991.